



Enhanced nonlinear optical characteristics of copper-ion-doped double crossover DNAs

Journal:	<i>Nanoscale</i>
Manuscript ID	NR-ART-07-2015-005075.R1
Article Type:	Paper
Date Submitted by the Author:	14-Sep-2015
Complete List of Authors:	<p>Park, Byeongho; Korea Institute of Science and Technology, Sensor System Center; Yonsei University, Mechanical Engineering</p> <p>Lee, Byung; Ajou University,</p> <p>Dugasani, Sreekantha Reddy; Sungkyunkwan University,</p> <p>Cho, Youngho; Kookmin University,</p> <p>Kim, Chulki; Korea Institute of Science and Technology,</p> <p>Seo, Minah; Korea Institute of Science and Technology, Sensor System Center</p> <p>Lee, Taikjin; Korea Institute of Science and Technology (KIST), Sensor System Research Center</p> <p>Jhon, Young; Korea Institute of Science and Technology, Sensor System Center</p> <p>Choi, Jaebin; Korea Institute of Science and Technology, Sensor System Center</p> <p>Lee, Seok; Korea Institute of Science and Technology, Sensor System Center</p> <p>Park, Sung Ha; Sungkyunkwan University, Department of Physics</p> <p>Jun, Seong Chan; Yonsei University, Mechanical Engineering</p> <p>Yeom, Dong-Il; Ajou Univ.,</p> <p>Rotermund, Fabian; Ajou University,</p> <p>Kim, Jae Hun; Korea Institute of Science and Technology, Sensor System Center</p>

Enhanced nonlinear optical characteristics of copper-ion-doped double crossover DNAs

*Byeongho Park^{1,2}, Byung Jic Lee³, Sreekantha Reddy Dugasani⁴, Youngho Cho^{1,5}, Chulki Kim¹, Minah Seo¹, Taikjin Lee¹, Young Min Jhon¹, Jaebin Choi¹, Seok Lee¹, Sung Ha Park⁴, Seong Chan Jun², Dong-Il Yeom³, Fabian Rotermund^{3**} and Jae Hun Kim^{1*}*

¹Sensor System Research Center, Korea Institute of Science and Technology (KIST), Seoul, Republic of Korea

²School of Mechanical Engineering, Yonsei University, Seoul, Republic of Korea

³ Department of Physics and Department of Energy Systems Research, Ajou University, Suwon, Republic of Korea

⁴Department of Physics and Sungkyunkwan Advanced Institute of Nanotechnology, Sungkyunkwan University, Suwon, Republic of Korea

⁵Departement of Bio and Nano Chemistry, Kookmin University, Seoul, Republic of Korea

Corresponding Authors

Corresponding authors: *jaekim@kist.re.kr and **rotermun@ajou.ac.kr

Present Addresses

*: Sensor System Research Center, Korea Institute of Science and Technology, 14-gil 5, Hwarang-ro, Seongbuk-gu, Seoul 136-130, Republic of Korea.

** : Department of Physics and Department of Energy Systems Research, Ajou University, 206, World cup-ro, Yeongtong-gu, Suwon 443-749, Republic of Korea

ABSTRACT

The modification of deoxyribonucleic acid (DNA) samples by sequencing the order of bases and doping copper ions opens the possibility for the design of novel nanomaterials exhibiting large optical nonlinearity. We investigated the nonlinear characteristics of copper-ion doped double crossover DNA samples for the first time to the best knowledge of authors by using Z-scan and four-wave mixing methods. To accelerate the nonlinear characteristics, we prepared two types of unique DNA nanostructures composed of 148 base pairs doped by copper ions with a facile annealing method. The outstanding third-order nonlinear optical susceptibility of the copper-ion-doped DNA solution, 1.19×10^{-12} esu, was estimated by the conventional Z-scan measurement, whereas the four-wave mixing experiment was also investigated. In the visible spectral range, copper-ion-doped DNA solution samples provided competent four-wave mixing signals with a remarkable conversion efficiency of -4.15 dB for the converted signal at 627 nm. The interaction between DNA and copper ions contributes to the enhancement of nonlinearity due to structural and functional changes. The present study signifies that the copper-ion-doped double crossover DNA is a potential candidate as a highly efficient novel material for further nonlinear optical applications.

Keywords : Copper ion, DNA, four-wave mixing, nonlinearity, Z-scan measurement

Introduction

Deoxyribonucleic acid (DNA) has become a fascinating material as a new photonic material due to its outstanding nonlinear optical property, whose unique structure with chirality contributes to the enhancement in optical nonlinearity¹⁻³. Several experiments have been previously performed to investigate the nonlinear characteristics of DNA. Based on Z-scan measurements, the nonlinear refractive index of DNA was determined by Samoc *et al.*⁴. Also, the third harmonic generation and degenerate four-wave mixing at 532 and 1064 nm were performed by using the functionalized DNA film⁵, which indicates that the third-order nonlinear optical susceptibility $\chi^{(3)}$ of the DNA film could be controlled according to the composition ratio of DNA and hexadecyltrimethylammonium-chloride (CTMA). The effect of chiral structure of DNA was also reported where the polarization of transmitting light was modulated⁶.

The current technology of DNA origami, the artificial rearrangement of bases, has allowed the engineering of individual bases in DNA leading to the variation of chemical and mechanical properties. Various nanocomposites such as PbS colloidal quantum dots in solution, silver on sapphire substrate and copper nanoclusters on silicate glass were also investigated to analyze their nonlinear optical properties.⁷⁻⁹ The intercalation of metal ions such as copper, nickel and zinc alters the optical property of DNA via band gap engineering¹⁰, while adding copper ions in the DNA has been known to induce the conformational change in DNA¹¹. Those DNA-based nanostructures have shown potential for developing novel biology-based electronics and optical applications in nanoscale. Previously, a copper oxide nano-sheet provided a high nonlinear refractive index of $-5.495 \times 10^{-11} \text{ m}^2/\text{W}$, measured by the Z-scan technique with a continuous-wave (cw) blue laser¹² and the third-order nonlinear optical property, $\chi^{(3)}/\alpha_0$, of the copper nanoparticles was estimated having a value in the range of $2.45 \times 10^{-12} \text{ esu}$ ¹³.

In this work, we prepared nanostructured DNAs doped with copper ions as a chiral platform in liquid to modify nonlinear optical characteristics. Our investigation of nonlinearity is based on Z-scan measurement providing Kerr nonlinearity. In addition, four-wave mixing has been studied for the applicable proof of high nonlinearity by copper-ion-doped DNAs.

Experimental

Four-strand entangled (Crossover) DNAs (DX_1 and DX_2) with 148 base pairs, the same as used in previous study (Fig. 1(a))^{10, 14}, were used for the investigation of their nonlinear optical characteristics in the present work. A single unit of the DX tile was organized such that two crossover junctions and two parallel duplexes are tied up by the junctions. The high-performance liquid chromatography (HPLC) purified synthetic oligonucleotides of DNA strands were acquired from Bioneer (Daejeon, Korea). DNA solutions were formed by mixing the stoichiometric quantity of eight different DNA strands (200 nM concentration) in a physiological $1\times$ TAE/ Mg^{2+} (40 mM Tris base, 20 mM Acetic acid, 1 mM EDTA (pH 8.0), and 12.5 mM magnesium acetate) buffer solution. The morphology of DNA samples was imaged by AFM (Digital Instruments Nanoscope III, Veeco, USA) with a multimode fluid cell head in a tapping mode under a buffer using NP-S oxide-sharpened silicon nitride tips (Veeco, USA) (Fig. 1(b)). DNA solution was annealed and cooled slowly down from 95°C to 25°C by placing an Axygen tube in a styrofoam box containing 2 L of boiled water for at least 24 hours to facilitate hybridization as shown in annealing part of Fig. 1(c). Copper ions $[Cu(NO_3)_2]$ at the concentration of 4 mM were added to the solution of the double crossover DNA followed by 24 hour incubation at room temperature (the second part of Fig. 1(c) for adding copper ion). To monitor the DNA lattice, 30 μ L of $1\times$ TAE/ Mg^{2+} buffer was dropped

onto a freshly cleaved mica surface, and then 5 μL of DNA solution was dropped onto the mica. Finally, this sample was placed onto the AFM stage.

We measured transmission and absorption from each of sample by spectrometer (Cary 5G spectrometer, Varian). For Z-scan measurement, mode-locked Ti:sapphire laser (Mai Tai Wideband, Spectra physics) was used to generate the high power beam. Four-wave mixing experimental setup was made by Ti:sapphire chirped pulse amplifier (CPA) system (Spitfire Ace-35F, Spectra physics) and optical parametric amplifier (OPA) (Topas prime, Spectra physics). The details of Z-scan measurement and four-wave mixing experiment are discussed in the following sections.

Results and discussion

In the spectral range between 300 and 1300 nm, all the samples exhibited negligible absorption as shown in Fig. 2. A shoulder peak around 260 nm, typically observed in the DNA samples^{4, 15, 16}, occurred in the copper-ion-doped DNA as well. It has been reported that copper ions can assist the enhancement in light absorption near 260 nm by the DNA-based complex solution¹⁰.

The refractive index of our samples in the visible-to-near infrared (VIS-to-NIR) range from 500 nm to 900 nm are represented in Fig. 3. The DNA solution presented gradually increasing refractive index with increasing the wavelength, while the copper-ion-doped DNA solution samples indicated a deep and a small valley around 600 and 800 nm, respectively.

To investigate the third-order nonlinearity of DNAs and the influence on nonlinearity by copper ion doping, Z-scan measurements were performed as shown in Fig. 4. A Ti:sapphire laser delivering 100-fs pulses at a repetition rate of 79.6 MHz was used as an excitation source. The output beam at 800 nm with the average power of 95 mW was focused by a convex lens delivering the beam waist of 14 μm in the focal plane. The corresponding peak intensity on the sample amounted to 3.4 GW/cm^2 . Each sample to be investigated was put in 1-mm-thick cuvette. Subsequently, the cuvette was

mounted on a computer-controlled translation stage and moved along the beam axis (z-axis) around the focal point to measure intensity-dependent nonlinear transmission changes through an aperture.

Figure 5 shows the closed-aperture Z-scan signals measured in different samples. The valley and peak curves imply an on-axis phase shift $\Delta\Phi$. Detected data (dots) can be fitted into the curve with the

transmittance function given by $T(x) = 1 + \frac{4x\Delta\Phi}{(1+x^2)(9+x^2)}$, where $x = -z/z_R$ is the normalized

distance from the focal point, and z_R is the Rayleigh length. From this function with measured data,

$\Delta\Phi$ is derived under the small distortion of the phase front and the sufficiently narrow closed aperture conditions. This approach provides comparable results such as the phase shift and the nonlinear characteristics among samples. The Kerr nonlinearity, γ , can be derived from the phase shift with

$\gamma = \Delta\Phi_0 / kI_0L_{eff}$, in which $k = 2\pi/\lambda$, I_0 is the intensity of light at the focus, and the L_{eff} is the

effective length of sample. The amplitude of nonlinear refractive index (n_2) can be written as

$$n_2 = n_0 c \gamma / 40\pi, \quad (1)$$

where c is the speed of light in vacuum, and n_0 is the linear refractive index. The third-order susceptibility including imaginary and real nature is presented as¹⁷

$$\chi^{(3)} = \sqrt{(\chi_I^{(3)})^2 + (\chi_R^{(3)})^2}, \quad (2)$$

$$\text{and } \chi_R^{(3)} = n_0^2 c \gamma / 120\pi^2. \quad (3)$$

Since our samples did not show any nonlinear absorption or saturation tendencies at 800 nm, the third-order susceptibility could be easily derived from the real part. In Table 1, the optical characteristics of copper-ion-doped DNA solution showed the largest nonlinearity compared to others since the copper ion plays a key role in the enhancement of optical nonlinearity.

It is worthy to note that the nonlinear Kerr coefficient of the copper-ion-doped DNA solution is about one order of magnitude larger than that of silicon waveguide, 4.5×10^{-15}

(cm^2/W), even if it is measured at 1550 nm wavelength¹⁸. In addition, the Kerr coefficient of the copper-ion-doped DNA solution is ten times larger than that of the previously reported DNA obtained from salmon roe, $\sim 10^{-15}$ (cm^2/W)⁴.

The schematic of four-wave mixing is shown in Fig. 6. The 100-fs output beam at 800 nm emitted from a 1-kHz Ti:sapphire CPA system is employed to pump an OPA for generation of two (signal and idler) beams at λ_1 and λ_2 . The signal and idler beams from OPA, which can be tuned from 1250 to 1575 nm and from 1650 to 2220 nm, respectively, are subsequently frequency-doubled in BBO crystal to achieve the signals in the VIS spectral region.

Linearly polarized input beams with intensities as high as about $5.36 \text{ GW}/\text{cm}^2$ at two different wavelengths, which are the second harmonic signals of two output beams emitted from the OPA, are focused on the sample in the tube using a parabolic mirror. After interaction over the path length of 6 mm, the generated four-wave mixing signal is measured by a monochromator with Si and PbS photo-detectors. Filters are used to eliminate undesired noise signals. When the visible light as an input beam is directed into the solution of DNA complex, the short pass filter at 1000 nm is used for blocking the infrared beams.

Photons in the incident beams at the wavelengths of λ_1 and λ_2 interact and generate electrons excited to an upper level at a higher energy. Transition from the excited state to the ground state emits the new photons as the third and fourth signals, which are given by following equations:

$$\lambda_3 = \frac{2\pi c}{\omega_3}, \quad \lambda_4 = \frac{2\pi c}{\omega_4} \quad (4)$$

$$\text{and } \omega_3 = 2\omega_1 - \omega_2, \quad \omega_4 = 2\omega_2 - \omega_1 . \quad (5)$$

The output signals created by four-wave mixing process follow the energy conservation rules represented in Eq. (5), which is called the phase-matching condition as

$$\omega_4 = \omega_1 + \omega_2 - \omega_3 \quad . \quad (6)$$

The transmitted spectrum in the VIS spectral range via copper-ion-doped DNA in solution is represented in Figs. 7 (a) and (b) for different input conditions. In Fig. 7(a), the signals at 728 nm (λ_1) and 897 nm (λ_2) generate two new beams at the wavelengths of 615 and 1138 nm, which agree well with the calculated third and fourth beams (λ_3 and λ_4) at 613 and 1168 nm from Eqs. (4) and (5) taking into account the coherent stokes and anti-stokes Raman processes^{19,20}. Input signals at the wavelengths of 742 and 876 nm are coupled into the solution sample and four different wavelength beams are detected as shown in Fig. 7(b). The peak positions of the third and fourth beams in the experiment are shown up at 627 and 1084 nm, which agree with the calculation results of 644 and 1069 nm. The propagation loss by coherent scattering in the solution and the variation of the group index due to the thermal shift of the beam wavelength are considered as follows:

$$\begin{aligned} \Delta k &= k_1 + k_2 - k_3 - k_4 \\ &= \frac{2\pi n_1}{\lambda_1} + \frac{2\pi n_2}{\lambda_2} - \frac{2\pi n_3}{\lambda_3} - \frac{2\pi n_4}{\lambda_4} \quad . \quad (7) \end{aligned}$$

Under the momentum conservation, the phase mismatching factor²¹⁻²³ was calculated by Eq. (7) with the refractive index of the complex of DNA and copper ions. The phase mismatching factors were -0.3475 and $-0.2890 \mu\text{m}^{-1}$ for the experimental results in Fig. 7(a) and (b). We note that the four-wave mixing shown in Fig. 7(b) appears to have higher efficiency than the case of Fig. 7(a) since the phase mismatch with the input beams of 742-876 nm is smaller than the one with 728-897 nm.

The conversion efficiency in four-wave mixing was derived from the experimental results by taking the ratio ($P_{\lambda_2} / P_{\lambda_3}$) between the output powers at wavelengths of λ_2 and λ_3 . The conversion efficiencies are -9.41 dB and -4.15 dB for the cases in Fig. 7(a) and (b). The experimental results

obtained in copper-ion-doped DNA solutions are three orders of magnitude larger than the previously reported results achieved in a typical silicon photonic crystal waveguide²⁴. The absorption in the liquid sample as shown in Fig. 2 contributed to generate unstable four-wave mixing signal in the IR range.

Using the signal at $\lambda_3 = 615$ nm, we compared the four-wave mixing efficiency among different samples as shown in Fig. 7(c). The intensity increased in the order of the buffer, DNA, copper-ion (4 mM), and copper-ion-doped DNA in the buffer solution. The nonlinear property of samples determined the third signal intensity near 615 nm. Increment in the intensity of newly generated waves is consistent with our Z-scan results shown in Table 1. This represents that copper-ion-doped DNA solution provides the highest four-wave mixing efficiency. The peak position shift shown in Fig. 7(c) was attributed to the different refractive indices of samples.

The optical characteristics of DNA is strongly sensitive to the structure of DNA itself that determines the polarizability affected by the incident photons^{25,26}. The electron transition in the purine and pyrimidine rings significantly contribute to the optical nonlinearity of DNA²⁷ and the reformed DNA conformation leads to the change of the dipole moment²⁸. Since both intrinsic copper and DNA possess interesting nonlinear characteristics, respectively, the four-wave mixing interaction of copper-ion-doped DNA is dramatically improved due to the additional structural change of DNA, in which the copper ions are located at the nucleosides. In this structural modification, copper ions play a key role in unwinding the bonding between DNA chains and disturbing the reformation of the hydrogen bond^{11,29}. The proper selections of the suitable buffer solution avoiding absorption in the sample will further lead to the substantial improvement in four-wave mixing interactions. DNA-based films adopting CTMA and DNA biopolymers³⁰ might be good candidates.

Conclusion

Our study verified that DNA, copper ions and copper-ion-doped DNA allow four-wave mixing process initiated by their enhanced third-order optical nonlinearity measured by Z-scan technique. By adding copper ions in DNA solution, the nonlinear property of DNA dispersed in solution was remarkably enhanced and the four-wave mixing efficiency was also improved because copper ions attribute to change DNA-based nanostructures, which modifies the optical property. According to phase mismatching factor with different input conditions, the efficiency of four-wave mixing was changed. While four-wave mixing in the near infrared (NIR) was disturbed by the unexpected absorption of buffer, stable four-wave mixing interaction was generated in the VIS with the small absorption of DNA and copper ion solution samples. Four-wave mixing in the DNA platform for signal amplification, frequency conversion, and regeneration will be very attractive in the field of integrated photonic circuits, considering it as a potential candidate in the futuristic biocompatible optical computing systems.

Acknowledgment

This work was partially supported by the Center for Advanced Meta-Materials (CAMM) as Global Frontier project (CAMM-NRF-2014M3A6B3063727 & CAMM-NRF-2014M3A6B3063709), the Nano Material Technology Development Program (2012M3A7B4049804), the Pioneer Research Center Program (2010-0019457), and the National Research Foundation of Korea (NRF) grant (2011-0017494) through the NRF funded by the Ministry of Science, ICT & Future Planning, and the KIST Institutional Program (Project No. 2E25382).

Authors' Contributions

Conceive and design the experiments

- Jae Hun Kim, Chulki Kim, Taikjin Lee, Young Min Jhon, Jaebin Choi, Seok Lee, Seong Chan Jun

Sample preparation

- Sreekantha Reddy Dugasani, Sung Ha Park

Experiments

- Byeongho Park, Youngho Cho, Byung Jic Lee, Minah Seo, Fabian Rotermund, Jae Hun Kim

Discussions

- Byeongho Park, Byung Jic Lee, Dong-Il Yeom, Fabian Rotermund, Jae Hun Kim

Writing

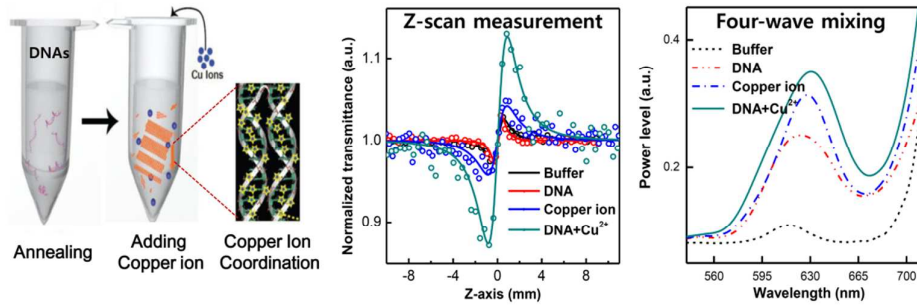
- Byeongho Park, Fabian Rotermund, Jae Hun Kim

Reference

1. R. W. Boyd, J. E. Sipe and P. W. Milonni, *Journal of Optics A: Pure and Applied Optics*, 2004, **6**, S14.
2. P. Fischer and F. Hache, *Chirality*, 2005, **17**, 421-437.
3. M. Samoc, A. Samoc, A. Miniewicz, P. P. Markowicz, P. N. Prasad and J. G. Grote, 2007.
4. M. Samoc, A. Samoc and J. G. Grote, *Chemical Physics Letters*, 2006, **431**, 132-134.
5. R. Czaplickia, O. Krupkaa, A. Megheab, J. Grotec, F. Kajzara and B. Sahraouia.
6. A. Kuzyk, R. Schreiber, Z. Fan, G. Pardatscher, E.-M. Roller, A. Hogege, F. C. Simmel, A. O. Govorov and T. Liedl, *Nature*, 2012, **483**, 311-314.
7. H. Cheng, Y. Wang, H. Dai, J.-B. Han and X. Li, *The Journal of Physical Chemistry C*, 2015, **119**, 3288-3292.
8. X.-x. Yu and Y.-h. Wang, *Opt. Express*, 2014, **22**, 177-182.
9. Y. H. Wang, Y. M. Wang, J. D. Lu, L. L. Ji, R. G. Zang and R. W. Wang, *Optics Communications*, 2010, **283**, 486-489.
10. S. R. Dugasani, T. Ha, B. Gnareddy, K. Choi, J. Lee, B. Kim, J. H. Kim and S. H. Park, *ACS Applied Materials & Interfaces*, 2014, **6**, 17599-17605.
11. G. L. Eichhorn and P. Clark, *Proceedings of the National Academy of Sciences of the United States of America*, 1965, **53**, 586.
12. M. Shahmiri, N. A. Ibrahim, N. Faraji, W. M. M. Yunus, N. Asim and N. Zainuddin, *Physica E: Low-dimensional Systems and Nanostructures*, 2013, **54**, 109-114.
13. R. A. Ganeev, A. I. Ryasnyansky, S. R. Kamalov, M. K. Kodirov and T. Usmanov, *Journal of Physics D-Applied Physics*, 2001, **34**, 1602-1611.
14. S. J. Kim, J. Jung, K. W. Lee, D. H. Yoon, T. S. Jung, S. R. Dugasani, S. H. Park and H. J. Kim, *ACS applied materials & interfaces*, 2013, **5**, 10715-10720.
15. J. Yguerabide and A. Ceballos, *Analytical biochemistry*, 1995, **228**, 208-220.
16. D. Xu, K. O. Evans and T. M. Nordlund, *Biochemistry*, 1994, **33**, 9592-9599.
17. H. H. Huang, F. Q. Yan, Y. M. Kek, C. H. Chew, G. Q. Xu, W. Ji, P. S. Oh and S. H. Tang, *Langmuir*, 1997, **13**, 172-175.
18. H. Tsang and Y. Liu, *Semiconductor Science and Technology*, 2008, **23**, 064007.
19. C. Thiel, *Journal*, 2011.
20. F. El-Diasty, *Vibrational Spectroscopy*, 2011, **55**, 1-37.
21. H. Zheng, X. Zhang, Z. Zhang, Y. Tian, H. Chen, C. Li and Y. Zhang, *Sci. Rep.*, 2013, **3**.
22. M. T. Turnbull, P. G. Petrov, C. S. Embrey, A. M. Marino and V. Boyer, *Physical Review A*, 2013, **88**, 033845.
23. K. O'Brien, H. Suchowski, Z. J. Wong, A. Salandrino, X. Yin and X. Zhang, 2014.
24. J. F. McMillan, M. Yu, D.-L. Kwong and C. W. Wong, *Optics Express*, 2010, **18**, 15484-15497.
25. J.-L. Mergny, J. Li, L. Lacroix, S. Amrane and J. B. Chaires, *Nucleic Acids Research*, 2005, **33**, e138-e138.
26. M. Govindaraju, H. Shekar, S. Sateesha, P. Vasudeva Raju, K. Sambasiva Rao, K. Rao and A. Rajamma, *Journal of Pharmaceutical Analysis*, 2013, **3**, 354-359.
27. E. Botek, F. Castet and B. Champagne, *Chemistry-A European Journal*, 2006, **12**, 8687-8695.
28. J. Bredas, C. Adant, P. Tackx, A. Persoons and B. Pierce, *Chemical Reviews*, 1994, **94**, 243-278.
29. P. Clark and G. L. Eichhorn, *Journal of Inorganic Biochemistry*, 1995, **59**, 765-772.
30. J. Zhou, Z. Y. Wang, X. Yang, C.-Y. Wong and E. Y. Pun, *Optics letters*, 2010, **35**, 1512-1514.

Graphical Abstract

Nonlinearity of double crossover DNAs investigated by Z-scan and four-wave mixing experiments was considerably enhanced with copper-ion doping.



Table

Table 1.

At 800 nm	Buffer	DNA	Copper ion	DNA+Cu ion
Refractive index (n_0)	1.3558	1.3826	1.3272	1.3452
Nonlinear Kerr coefficient (γ) [cm^2/W]	2.11×10^{-15}	2.26×10^{-15}	8.65×10^{-15}	2.59×10^{-14}
Third-order nonlinear susceptibility ($\chi^{(3)}$) [esu]	9.82×10^{-14}	1.09×10^{-13}	3.86×10^{-13}	1.19×10^{-12}
Nonlinear refractive index (n_2) [esu]	6.83×10^{-13}	7.46×10^{-13}	2.74×10^{-12}	8.32×10^{-12}

Table caption

Table 1: Optical characteristics of 1×TAE/Mg²⁺ buffer, only DNA, only copper ion, and copper-ion-doped DNA solutions including linear refractive index, nonlinear Kerr coefficient, third-order nonlinear susceptibility, and nonlinear refractive index.

Figure captions

Figure 1: (a) Sequence map for two types of the double crossover (DX) structure (DX1, and DX2 tiles). Each tile consisted of four strands and the complementary sticky end pairs are shown as S_n and S_n' ($n = 1, 2, 3, 4$) in the sequence drawings (violet). (b) The measured AFM (Atomic Force Microscopy) image, noise-filtered and reconstructed by fast Fourier transform, represents the clear periodicity of the DX crystals. (c) Schematics of DNA free solution annealing, Cu ion doping into DNA lattice after annealing, and Cu ion coordination sites in DX structure.

Figure 2: Absorption spectra of samples: $1\times\text{TAE}/\text{Mg}^{2+}$ buffer, only DNA, only copper ion, and copper-ion-doped DNA solutions. Scale up view of absorption spectra from 220 to 375 nm (inset).

Figure 3: Refractive index of (a) DNA and (b) copper-ion-doped DNA solutions with different concentrations.

Figure 4: Schematic of Z-scan measurement based on femtosecond laser.

Figure 5: Z-scan traces measured in samples with $1\times\text{TAE}/\text{Mg}^{2+}$ buffer, only DNA, only copper ion, and copper-ion-doped DNA solutions. Dots are recorded data and lines fitted curves.

Figure 6: Experimental setup of four-wave mixing based on OPA pumped by 1-kHz Ti:sapphire CPA system. Silver protected parabolic mirror was employed to focus the input beam into solution sample, and convex lens was used for collecting the output beams for detection by monochromator. A test tube open at both beam-incident and beam-exit surfaces holding liquid DNA solution by surface tension is directly exposed to input beams (inset).

Figure 7: Four-wave mixing results of $1\times\text{TAE}/\text{Mg}^{2+}$ buffer, only DNA, only copper ion, copper-ion-doped DNA solutions. Four-wave mixing results in the VIS and NIR spectral region with four-different input conditions, achieved in copper-ion-doped DNA solution: (a) 728-897 nm and (b) 742-

876 nm. λ_1 and λ_2 are input beams and λ_3 and λ_4 are newly generated beams by four-wave mixing. (c) Four-wave mixing results enlarged at third beam near 615 nm to compare conversion efficiency of four-wave mixing interaction among samples, $1\times\text{TAE/Mg}^{2+}$ buffer (black), only DNA (red), only copper ion (blue), and copper- ion-doped DNA (green) in buffer solution.

Figure 1.

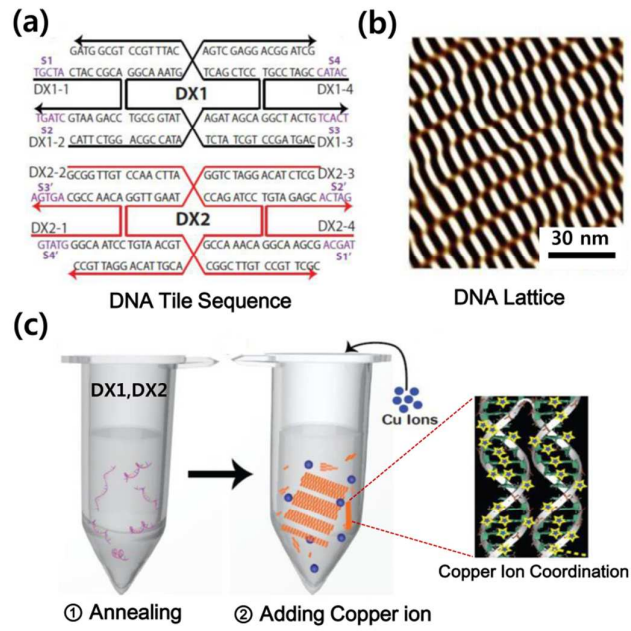


Figure 2.

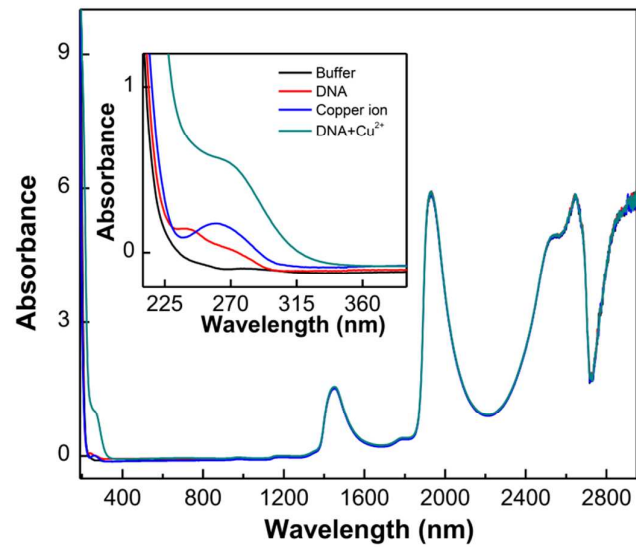


Figure 3.

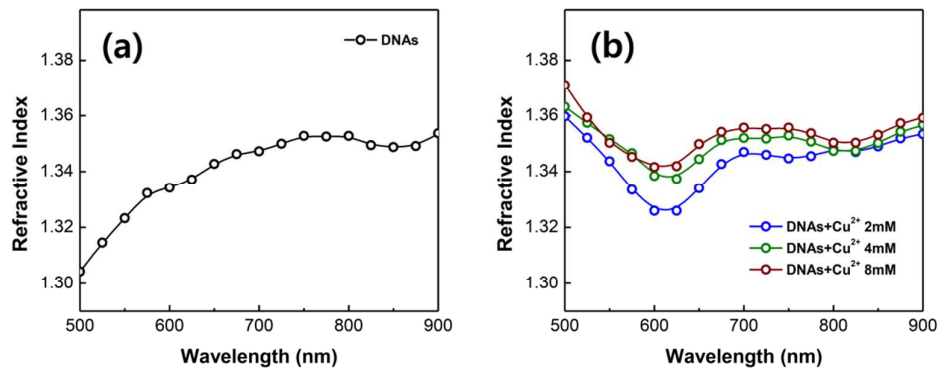


Figure 4.

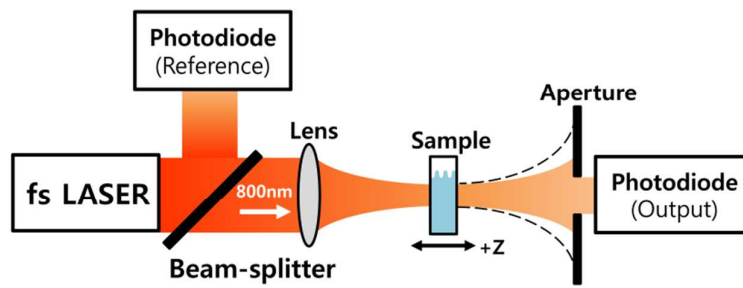


Figure 5.

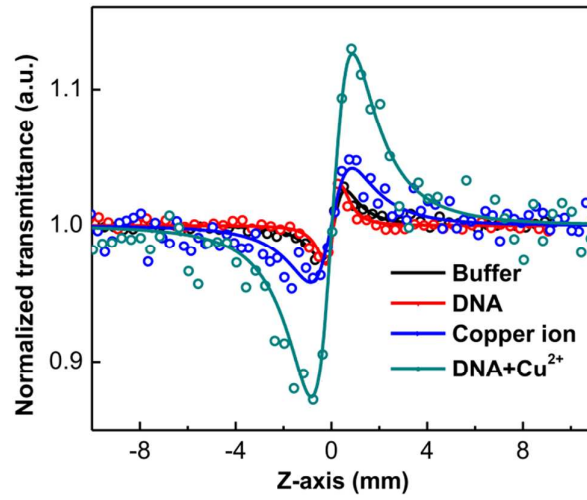


Figure 6.

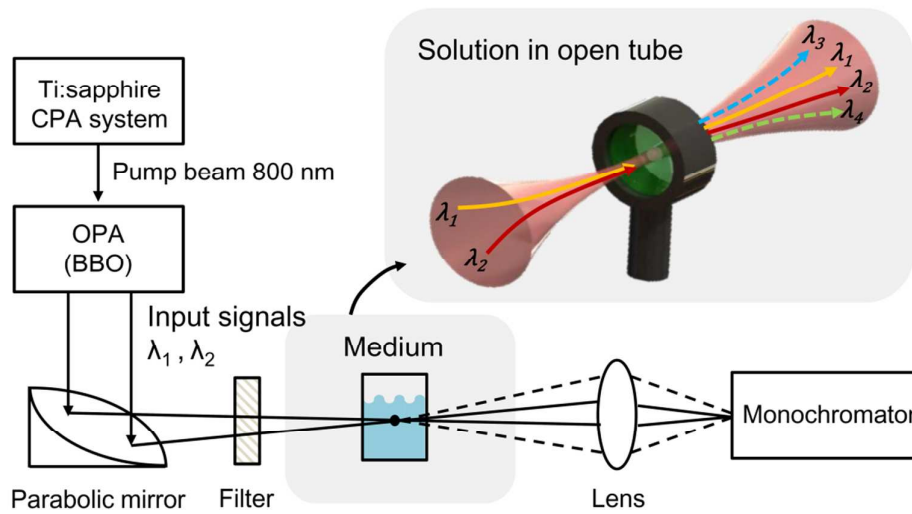


Figure 7.

